Inventory of Supplemental Information presented in relation to each of the main figures in the manuscript

Supplemental Data

1. **Figure S1**. Related to Figure 1.

2. **Figure S2.** Related to Figure 2.
3. **Table S1.** Related to Figure 2.

4. **Figure S3.** Related to Figure 3.
5. **Table S2.** Related to Figure 3.
6. **Table S3.** Related to Figure 3.
7. **Table S4.** Related to Figure 3.

8. **Figure S4.** Related to Figure 4.

9. **Figure S5.** Related to Figure 5.

Supplemental Experimental Procedures

1. Expression profiling data processing
2. Real-time quantitative PCR
3. Erythroid colony processing for flow cytometry, immunocytochemistry and immunoblotting
4. Cell line cultures and transfection
5. Plasmid constructions and lentivirus production
6. K562 differentiation assays
7. Cord blood $CD34^+$ MNC purification and erythroid/megakaryocytic differentiation
8. Western blot analyses

Supplemental References (3)

Figure S1

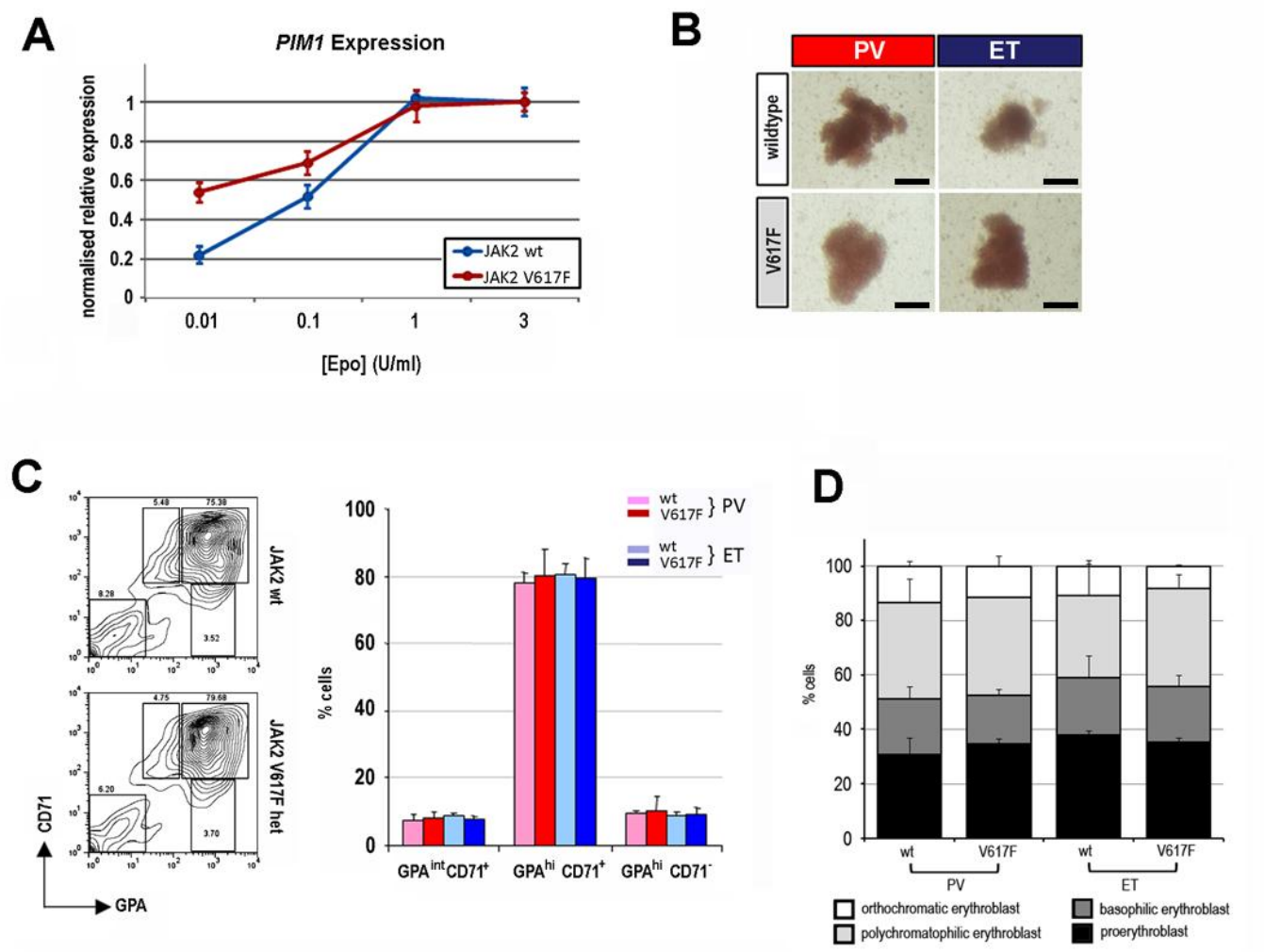

Figure S1, related to Figure 1.

(A) Analysis of *PIM1* expression by quantative RT-PCR in wild-type and V617F-heterozygous BFU-e colonies grown at 0.01, 0.1, 1 and 3 U/ml erythropoietin (EPO). Levels of *PIM1* transcripts for each colony genotype are shown relative to expression in colonies grown at 3 U/ml EPO. Significant differences in expression between wild-type and V617F-heterozygous BFU-E's were observed only in colonies grown at 0.01 and 0.1 U/ml EPO. All PCRs were standardized to β-actin and performed in triplicate. Each point represents the mean ± S.D. for 3 independent reactions.

(B) Representative colonies from wild-type and V617F-heterozygous BFU-E's from PV and ET patients. No obvious differences in colony size or morphology were observed. Scale bars indicate 50 μm.

(C) FACS analyses assessing expression of glycophorin A (GPA) and CD71 in wild-type and V617F-heterozygous BFU-E's grown at 0.01 U/ml EPO. No significant differences were observed in the percentages of $GPA^{int}CD71^{+}$, $GPA^{hi}CD71^{+}$ and $GPA^{hi}CD71^{-}$ subpopulations between the two colony genotypes in PV and ET patients. The results represent the mean ± S.D. for 3 PV and 3 ET patients.

(D) Cells of the erythroid series were scored from cytospins generated from wild-type and V617-heterozygous BFU-E's pooled from 2 PV and 2 ET patients. No differences in the proportion of cells at the different stages of erythroid differentiation were observed. Black bar: proerythbolast; dark grey: basophilic erythroblast, light grey: polychromatophilic erythroblast; white: orthochromatic erythroblast. Error bars denote standard deviation.

Figure S2

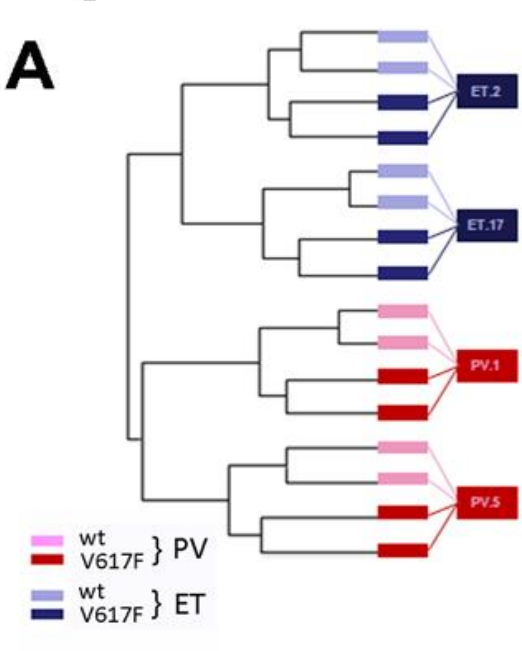

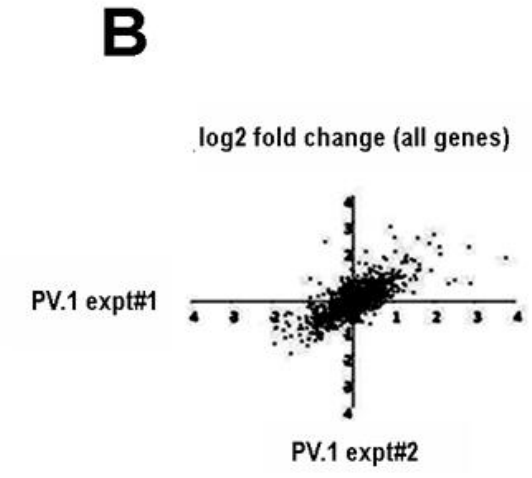

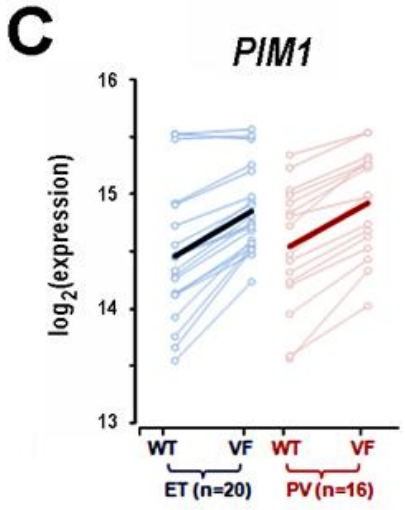

PIM1	RHBDD2	LOC651369	TRIM15	POMZP3	THRA	RPL23AP7
SOCS3	PLA2G4C	JMJD2B	NIFUN	LOC645236	RELB	CDC2L2
CISH	FAM83A	LOC641825	HS.497591	KCNK3	HIST1H1C	RECQL5
SOCS2	HSPA6	TMEM16K	USP36	GMPPB	FLJ21749	ATPBD3
CCND2	MGC24381	ASPSCR1	TNFSF9	KIAA1632	IIP45	SCO2
PHKG2	TULP3	FAM96B	HS.58896	HS.549989	HYPE	HS.19339
CD80	SLC25A34	KIAA1602	RNU35B	HS.568329	SYMPK	FAM22A
GABARAP	IFI30	SPOCK2	HS.559654	STK40	DUSP5	CD14
LENG4	HS.143018	ID1	LOC647512	FLJ22688	GDPD3	DUSP3
TMPIT	FAM83A	LOC643009	HERC5	ABCF3	CCNT2	PFDN6
TRIM15	HS.574968	RNF185	KSR1	GSTO2	HS.571622	PCSK1N
DHDH	MAX	LOC90321	PHLDA3	SSSCA1	LOC641808	LOC440345
HS.396795	LTB4R	SESN2	C19ORF24	EGR1	CLEC2B	PLEKHB2
HS.543842	PVRL2	STK11IP	MOCOS	C3ORF60	S100P	LOC642441
HSPA5	HIST2H2AC	LOC388574	NOL10	FLJ35725	RRAD	FOSL1
KLF6	CDKN1A	ZNF346	HS.535360	FLJ10815	DKFZP586I1420	FLJ25778
ESR2	PLCG1	HS.288735	MAX	XPA	FKBP4	SFXN5
HS.234961	LOC642393	TUBB3	SLC45A4	UPK1A	HS.547201	IDS
ASS	PLEKHA4	LOC146177	FLJ40142	DUSP26	C17ORF68	USMG5
FLJ20366	PHF1	CPT1B	HIST2H2BE	MGC16121	SLC37A1	AASS
IL10RA	PIM3	FAM112B	FKSG24	SAC	TRIM9	DLG5
H3F3B	LOC653610	LOC619383	PHGDH	SOD2	CLN8	HS.197143
HS.170035	BCL2L1	ST3GAL4	TICAM1	LOC389901	LOC115098	CHAC1
ZFAND2A	PHF7	PRR7	KIAA1683	LOC642033	CARD9	LOC652598
OPLAH	ASGR1	CTRL	FRAT1	PSMB8	LOC113179	DIRC2
WDR25	C8ORF48	HS.568148	C16ORF5	FOXP1	IFI27	POU2F1
C10ORF10	C19ORF28	HS.171171	HS.580740	OSCAR	LOC441150	
LOC147808	C9ORF37	HS.562701	TAP1	FAIM3	POLR3D	
TNKS	GPX3	HS.120058	DAPK1	LOC653382	LOC58489	

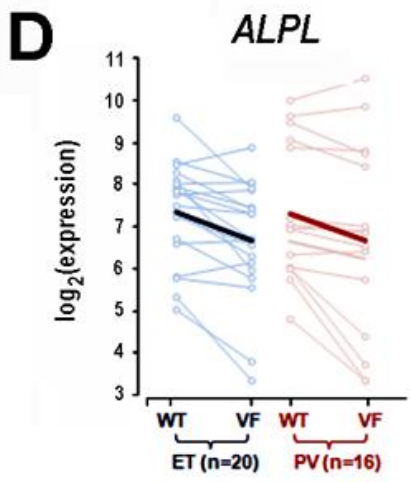

YBX2	SEH1L	SLC25A20	LOC644774
ALPL	SP4	TMEM14A	LOC399942
SNCA	ECOP	NETO2	THOC4
RAVER2	KIT	CASC4	LOC643995
LOC648517	PAQR9	MGC18216	
BCL6	SLC2A14	ARHGAP23	

Figure S2, related to Figure 2.

(A) Hierarchical clustering of expression profiles generated from initial and repeat samples derived from 2 ET and 2 PV patients. Datasets from PV patients (PV.1 and PV.5) are depicted as light red for expression profiles from wild-type erythroblasts and dark red for expression profiles from V617F-heterozygous erythroblasts, with each patient connected by a line to their four expression profiles. Datasets for ET patients (ET.2 and ET.17) are similarly depicted as light blue for expression profiles from wild-type erythroblasts and dark blue for expression profiles from V617F-heterozygous erythroblasts.

(B) Log-log scatter plot comparison of gene expression patterns for all genes (expressed as log2-ratio of expression in V617F-heterozygous relative to autologous wild-type erythbroblasts) in independently run experiments for patient PV.1 reveals strong concordance in expression profile.

(C) List of 201 genes exhibiting up-regulation in V617F-heterozygous erythroblasts relative to autologous wild-type controls across all samples irrespective of MPN subtype (minimum fold change, 1.3; p-values $\leq$ 0.0034). Interaction plot depicting increased expression of a representative gene *PIM1* in V617F-heterozygous erythroblasts relative to autologous wild-type controls is shown. For each individual, the gene expression as measured on the microarrays is shown for wild-type (WT) and V617F-heterozygous (VF) erythroblasts, and the corresponding values are connected by solid lines. Individual ET patients are depicted in light blue, individual PV patients are depicted in light red, and the average of all patients for each disease type shown overlayed using a dark line.

(D) List of 22 genes exhibiting down-regulation in V617F-heterozygous erythroblasts relative to autologous wild-type controls across all samples irrespective of MPN subtype (minimum fold change, 1.3; p-values $\leq$ 0.0034). Interaction plot depicting decreased expression of a representative gene, *ALPL*, is shown, as described above.

Table S1, related to Figure 2. Clinical details of MPN patients studied.

Feature	PV (n=16)	ET (n=20)	p
Demographic Characteristics			
Male Sex - no. (%)	8 (50)	10 (50)	1.0
Median age at diagnosis - yr (range)	63 (12-80)	58 (29-90)	0.8
Laboratory and clinical features at diagnosis			
Hemoglobin - g/litre			
Mean	181 ± 23	142 ± 11	< 0.0001
Median (range)	181 (128-225)	144 (121-162)	
Platelet count - $x10^{-3}/mm^3$			
Mean	618 ± 297	933 ± 362	0.01
Median (range)	555 (138-1139)	811 (544-2030)	
Neutrophil count - $x10^{-3}/mm^3$			
Mean	8.2 ± 2.8	6.2 ± 1.6	0.03
Median (range)	8.1 (2.4-13.6)	6.1 (3.2-10.2)	
Laboratory and clinical features /at sample collection			
Median disease duration - mo. (range)	35 (0-158)	23 (2-102)	0.3
Treatment - no. (%)			
None	1 (6)	0 (0)	0.3
Aspirin or other antiplatelet agent only	3 (19)	9 (45)	0.1
Hydroxyurea	12 (75)	10 (50)	0.1
Anagrelide	0 (0)	1 (5)	0.4

Figure S3

A

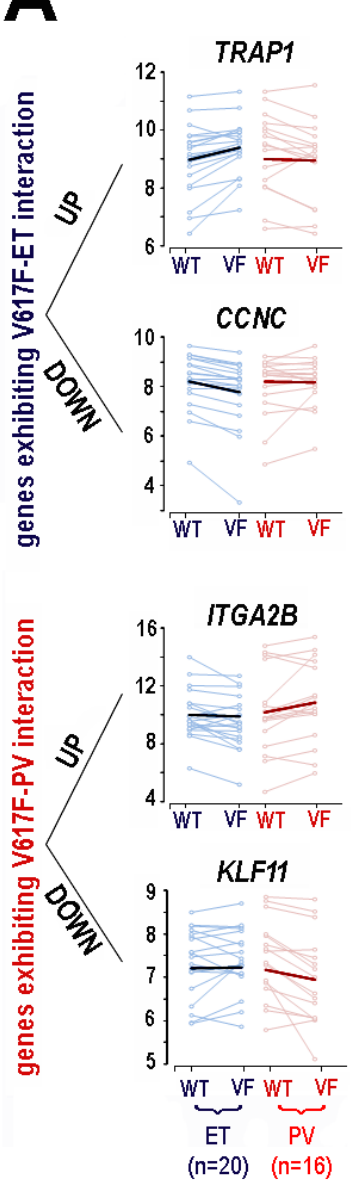

HLA-DRB1	POLRMT	VASH1	PHF15	BRMS1	FBXO31	GNL1
OAS2	SLC7A6OS	NELF	DFFA	ALDOC	ADRM1	ST3GAL1
PLA2G4C	WDR74	CKB	MPZL1	PYGB	EPN1	PRMT5
GBP1	HLA-H	RPS6KB2	TBC1D7	ARD1A	LOC112869	MFSD5
OAS1	TMEM16K	HMHA1	REXO1	HLA-F	PFKL	CPSF3L
CTXN1	IFIT2	C1ORF164	BCKDHA	AVPI1	SIAHBP1	AFG3L2
ABHD14B	IRF7	IFITM1	NULP1	SLC9A1	LHPP	SNAPC2
LOC113179	IFITM2	FLJ10374	EMD	NUDC	UCKL1	IRF1
IFI44L	IFIT3	HLA-DQA1	GTPBP6	BANP	CHD4	ZNF672
TRAP1	SLC25A22	ZNHIT4	DPAGT1	FARSLA	RNMTL1	EVL
MX1	P2RY11	IFITM3	IDH3B	FLJ10241	GNPDA1	PPRC1
GBP2	FLJ11286	GANAB	DAXX	SUPV3L1	TMEM101	

(i)

TMED5	ZNF189	NDUFA4	SNX2	HERC4	ESD
NGLY1	LOC644799	CHMP5	APAF1	MYNN	
CCNC	ARFGEF1	GTF2E1	GGPS1	UQCRB	
NUMB	BNIP2	PIGK	SUDS3	COMMD10	

(ii)

HS.407903	STK3	C1GALT1C1	JMJD1C	ATP6AP2	TMEM77
CEBPD	NDUFB5	RPS27L	KLHL2	ZNF198	PCTK2
ITGA2B	AZI2	GALC	RASGRP3	HS.130036	PEX19
FPR1	NCOA4	RUNDC1	SELT	VPS29	C6ORF62
SUDS3	CNIH4	SNX16	COMMD2	NPC2	LRRC37B
C15ORF26	RAP2C	RICTOR	RAB10	SLC35B3	FLJ10726
ZNF585A	RAD23B	EXOC1	LSM8	C14ORF100	ETNK1

(iii)

MED25	SERINC2	EIF5A	LMNA	FANCE	THAP11
LGTN	GCN5L2	UBE2I	TBC1D4	RSL1D1	KLHDC3
FBL	SLC41A1	PPM1G	KLF11	NOL1	XRCC6
EEF2	ATP6V0E2L	ACSS1	IMPDH2	SF3B4	

(iv)

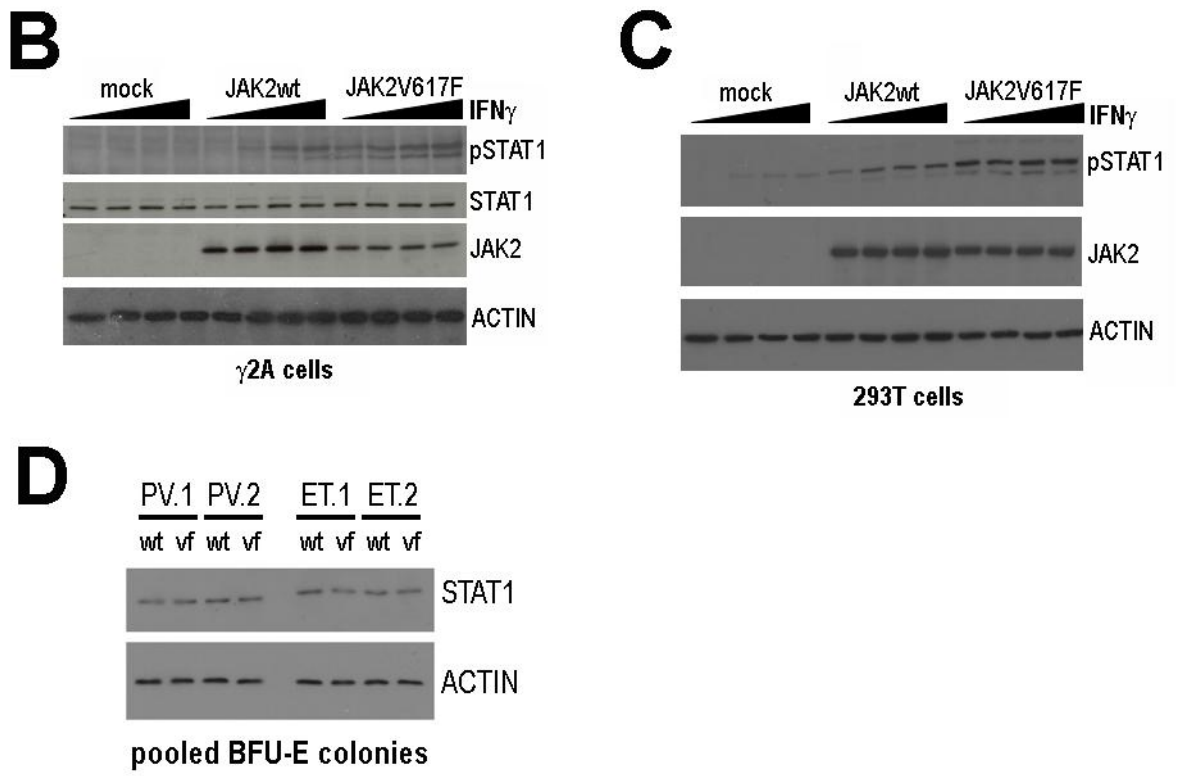

Figure S3, related to Figure 3.

(A) List of 171 genes exhibiting significant interaction between the *JAK2V617F* mutation and disease subtype which fell into four groups defined by their patterns of behavior. For genes exhibiting significant interaction between the *JAK2V617F* mutation and ET, 83 genes were up-regulated in mutant erythroblasts (i), and 21 genes were down-regulated in mutant erythroblasts (ii). For genes exhibiting significant interaction between the *JAK2V617F* mutation and PV, 40 genes were up-regulated in mutant erythroblasts (iii), and 24 genes were down-regulated in mutant erythroblasts (iv). Interaction plots depicting a representative gene from each of these four groups (i-iv) are shown. For each individual, the gene expression as measured on the microarrays is shown for wild-type (WT) and V617F-heterozygous (VF) erythroblasts, and the corresponding values are connected by solid lines. Individual ET patients are depicted in light blue, individual PV patients are depicted in light red, and the average of all patients for each disease type shown overlayed using a dark line.

(B) Western immunoblot analyses of JAK2-null γ2A cells mock transfected or transfected with either wild-type JAK2 or JAK2V617F and treated with 0, 1, 10 and 100 ng/ml IFNγ for 15'. Elevated STAT1 phosphorylation on tyrosine-701 is seen in JAK2V617F-transfected cultures at all doses tested.

(C) Analysis of pSTAT1 levels in 293T cells transfected with wild-type JAK2 or JAK2V617F and treated with 0, 1, 10 and 100 ng/ml IFNγ for 15' shows similar phosphorylation of STAT1 on tyrosine-701.

(D) Analysis of total STAT1 levels in wild-type JAK2 or JAK2V617F erythroblasts cultured in 0.01 U/ml Epo. No appreciable difference in total STAT1 levels was detected in mutant erythroblasts relative to autologous wild-type erythroblasts in both PV and ET.

Table S2, related to Figure 3. Gene Set Enrichment Analysis – V617F-ET interacting genes

GENE SET NAME	BRIEF DESCRIPTION	ENRICH-MENT SCORE	p-value	FDR q-value
UVC_TTD_4HR_UP	Up-regulated at 4 hours following treatment of XPB/TTD fibroblasts with 3 J/m^2 UVC	-2.20	<0.001	0.001
BRCA1_OVEREXP_DN	Downregulated by induction of exogenous BRCA1 in EcR-293 cells	-2.16	<0.001	0.002
IFNALPHA_HCC_UP	**Upregulated by interferon alpha treatment in Hep3B hepatocellular carcinoma cells**	**-2.06**	**<0.001**	**0.006**
MYC_ONCOGENIC_SIGNATURE	Genes selected in supervised analyses to discriminate cells expressing c-Myc oncogene	-2.03	<0.001	0.007
IFNALPHA_NL_HCC_UP	**Upregulated by interferon alpha treatment in both normal primary hepatocytes and Hep3B hepatocellular carcinoma cells**	**-2.00**	**<0.001**	**0.009**
BRCA2_BRCA1_UP	Genes up-regulated in BRCA2-linked breast tumors, relative to BRCA1-linked tumors	-1.98	<0.001	0.011
CROMER_HYPOPHARYNGEAL_MET_VS_NON_DN	Genes increased in non-metastatic hypopharyngeal cancer tumours	-1.87	<0.001	0.033
UVC_TTD_ALL_UP	Up-regulated at any timepoint following treatment of XPB/TTD fibroblasts with 3 J/m^2 UVC	-1.85	<0.001	0.035
INOS_ALL_DN	Downregulated following iNOS induction in hepatocytes	-1.85	0.002	0.034
IFNALPHA_NL_UP	**Upregulated by interferon alpha treatment in both normal primary hepatocytes**	**-1.81**	**<0.001**	**0.044**
PENG_GLUTAMINE_DN	Genes downregulated in response to glutamine starvation	-1.79	<0.001	0.049
RADAEVA_IFNA_UP	**Genes up-regulated by interferon-alpha in primary hepatocyte**	**-1.78**	**<0.001**	**0.052**
BRENTANI_TRANSCRIPTION_FACTOR	Cancer related genes that are also transcription factors	-1.75	0.002	0.065
REOVIRUS_HEK293_DN	Down-regulated at any timepoint up to 24 hours following infection of HEK293 cells with reovirus strain T3Abney	-1.74	<0.001	0.067
CHEN_HOXA5_TARGETS_DN	Genes down-regulated in response to HOXA5 expression	-1.73	0.006	0.066

TNFALPHA_30MIN_UP	Upregulated 30min after TNF-alpha treatment of HeLa cells	-1.72	0.009	0.066
IFN_ALL_UP	**Upregulated 2-fold in HT1080 cells 6 hours following treatment with interferons alpha, beta and gamma**	**-1.71**	**0.005**	**0.070**
PENG_LEUCINE_DN	Genes downregulated in response to leucine starvation	-1.65	<0.001	0.114
WALLACE_JAK2_DIFF	JAK2-dependent genes with a 7-fold change relative to JAK2-null cells	-1.60	0.022	0.154
IFN_GAMMA_UP	**Upregulated 2-fold in HT1080 cells 6 hours following treatment with interferon gamma**	**-1.60**	**0.005**	**0.152**
GALINDO_ACT_UP	Most significant genes up-regulated by Act in macrophages	-1.59	0.009	0.155
IFN_ALPHA_UP	**Upregulated 2-fold in HT1080 cells 6 hours following treatment with interferon alpha**	**-1.57**	**0.011**	**0.169**
MOREAUX_TACI_HI_VS_LOW_UP	Genes overexpressed in TACI high patients	-1.56	0.002	0.172

Table S3, related to Figure 3. Gene Set Enrichment Analysis – V617F-PV interacting genes

GENE SET NAME	BRIEF DESCRIPTION	ENRICH-MENT SCORE	p-value	FDR q-value
UVC_TTD_4HR_DN	Down-regulated at 4 hours following treatment of XPB/TTD fibroblasts with 3 J/m^2 UVC	2.34	<0.001	0.012
POD1_KO_DN	Down-regulated in glomeruli isolated from Pod1 knockout mice versus wild-type controls	2.33	<0.001	0.006
AGED_MOUSE_ HYPOTH_UP	Up-regulated in the hypothalamus of aged (22 months) BALB/c mice, compared to young (2 months) BALB/c mice	2.32	<0.001	0.004
UVC_XPCS_ALL_ DN	Down-regulated at any timepoint following treatment of XPB/CS fibroblasts with 3 J/m^2 UVC	2.31	<0.001	0.003
UVC_XPCS_4HR_ DN	Down-regulated at 4 hours following treatment of XPB/CS fibroblasts with 3 J/m^2 UVC	2.29	<0.001	0.005
UVC_XPCS_8HR_ DN	Down-regulated at 8 hours following treatment of XPB/CS fibroblasts with 3 J/m^2 UVC	2.24	<0.001	0.008
UVC_TTD_ALL_DN	Down-regulated at any timepoint following treatment of XPB/TTD fibroblasts with 3 J/m^2 UVC	2.23	<0.001	0.007
UVC_HIGH_ALL_DN	Down-regulated at any timepoint following treatment of WS1 human skin fibroblasts with UVC at a high dose UVC	2.21	<0.001	0.006
UVC_HIGH_D2_DN	Down-regulated at day 2 following treatment of WS1 human skin fibroblasts with UVC at a high dose UVC	2.11	<0.001	0.025
BRCA1KO_MEF_DN	Down-regulated in mouse embryonic fibroblasts following targeted deletion of BRCA1	2.09	<0.001	0.034
REOVIRUS_HEK293 _UP	Up-regulated at any timepoint up to 24 hours following infection of HEK293 cells with reovirus strain T3Abney	2.09	<0.001	0.032
UVB_NHEK1_DN	Downregulated by UV-B light in normal human epidermal keratinocytes	2.09	<0.001	0.029
CHEN_HOXA5_ TARGETS_UP	Genes up-regulated in response to HOXA5 expression	2.07	<0.001	0.040

FLECHNER_KIDNEY_TRANSPLANT_WELL_UP	Genes upreglated in well functioning transplanted kidney biopsies from stable immunosuppressed recipients	2.02	<0.001	0.060
AGEING_BRAIN_UP	Genes upregulated in the human frontal cortex with ageing	2.01	<0.001	0.070
TAKEDA_NUP8_HOXA9_8D_DN	Genes down-regulated at 8 days following expression of NUP98-HOXA9 in CD34+ human hematopoietic stem cells	1.99	<0.001	0.088
ALZHEIMERS_DISEASE_DN	Downregulated in correlation with overt Alzheimer's Disease	1.99	<0.001	0.085
DIAB_NEPH_DN	Downregulated in the glomeruli of cadaver kidneys from patients with diabetic nephropathy	1.97	<0.001	0.097
UVC_HIGH_D4_DN	Down-regulated at day 4 following treatment of WS1 human skin fibroblasts with UVC at a high dose UVC	1.96	<0.001	0.100
UVB_NHEK3_C2	Regulated by UV-B light in normal human epidermal keratinocytes	1.96	0.002	0.102
GREENBAUM_E2A_UP	Transcripts up-regulated 3-fold or greater in the E2A-deficient cell lines	1.91	<0.001	0.167
UVC_HIGH_D3_DN	Down-regulated at day 3 following treatment of WS1 human skin fibroblasts with UVC at a high dose UVC	1.91	<0.001	0.168
BRCA1_OVEREXP_UP	Upregulated by induction of exogenous BRCA1 in EcR-293 cells	1.90	<0.001	0.166
UVC_TTD-XPCS_COMMON_DN	Down-regulated at any timepoint following treatment of both XPB/CS and XPB/TTD fibroblasts with 3 J/m^2 UVC	1.90	<0.001	0.161
UVB_SCC_UP	Upregulated by UV-B light in squamous cell carcinoma cells	1.88	0.002	0.190

Table S4, related to Figure 3. Interferon responsive genes in JAK2V617F targets.

		type I	type II
	HLA-DRB1		
Genes up-regulated in V617F cells specifically in ET	OAS2		
	PLA2G4C		
	GBP1		
	OAS1		
	CTXN1		
	ABHD14B		
	LOC113179		
	IFI44L		
	TRAP1		
	MX1		
	GBP2		
	POLRMT		
	SLC7A6OS		
	WDR74		
	HLA-H		
	TMEM16K		
	IFIT2		
	IRF7		
	IFITM2		
	IFIT3		
	SLC25A22		
	P2RY11		
	FLJ11286		
	VASH1		
	NELF		
	CKB		
	RPS6KB2		
	HMHA1		
	C1ORF164		
	IFITM1		
	FLJ10374		
	HLA-DQA1		
	ZNHIT4		
	IFITM3		
	GANAB		
	PHF15		
	DFFA		
	MPZL1		
	TBC1D7		
	REXO1		
	BCKDHA		
	NULP1		
	EMD		
	GTPBP6		
	DPAGT1		
	IDH3B		
	DAXX		
	BRMS1		
	ALDOC		
	PYGB		
	ARD1A		
	HLA-F		
	AVPI1		
	SLC9A1		
	NUDC		
	BANP		
	FARSLA		
	FLJ10241		
	SUPV3L1		
	FBXO31		
	ADRM1		
	EPN1		
	LOC112869		
	PFKL		
	SIAHBP1		
	LHPP		
	UCKL1		
	CHD4		
	RNMTL1		
	GNPDA1		
	TMEM101		
	GNL1		
	ST3GAL1		
	PRMT5		
	MFSD5		
	CPSF3L		
	AFG3L2		
	SNAPC2		
	IRF1		
	ZNF672		
	EVL		
	PPRC1		

		type I	type II
Genes up-regulated in V617F cells specifically in PV	HS.407903		
	CEBPD		
	ITGA2B		
	FPR1		
	SUDS3		
	C15ORF26		
	ZNF585A		
	STK3		
	NDUFB5		
	AZI2		
	NCOA4		
	CNIH4		
	RAP2C		
	RAD23B		
	C1GALT1C1		
	RPS27L		
	GALC		
	RUNDC1		
	SNX16		
	RICTOR		
	EXOC1		
	JMJD1C		
	KLHL2		
	RASGRP3		
	SELT		
	COMMD2		
	RAB10		
	LSM8		
	ATP6AP2		
	ZNF198		
	HS.130036		
	VPS29		
	NPC2		
	SLC35B3		
	C14ORF100		
	TMEM77		
	PCTK2		
	PEX19		
	C6ORF62		
	LRRC37B		
	FLJ10726		
	ETNK1		

Figure S4

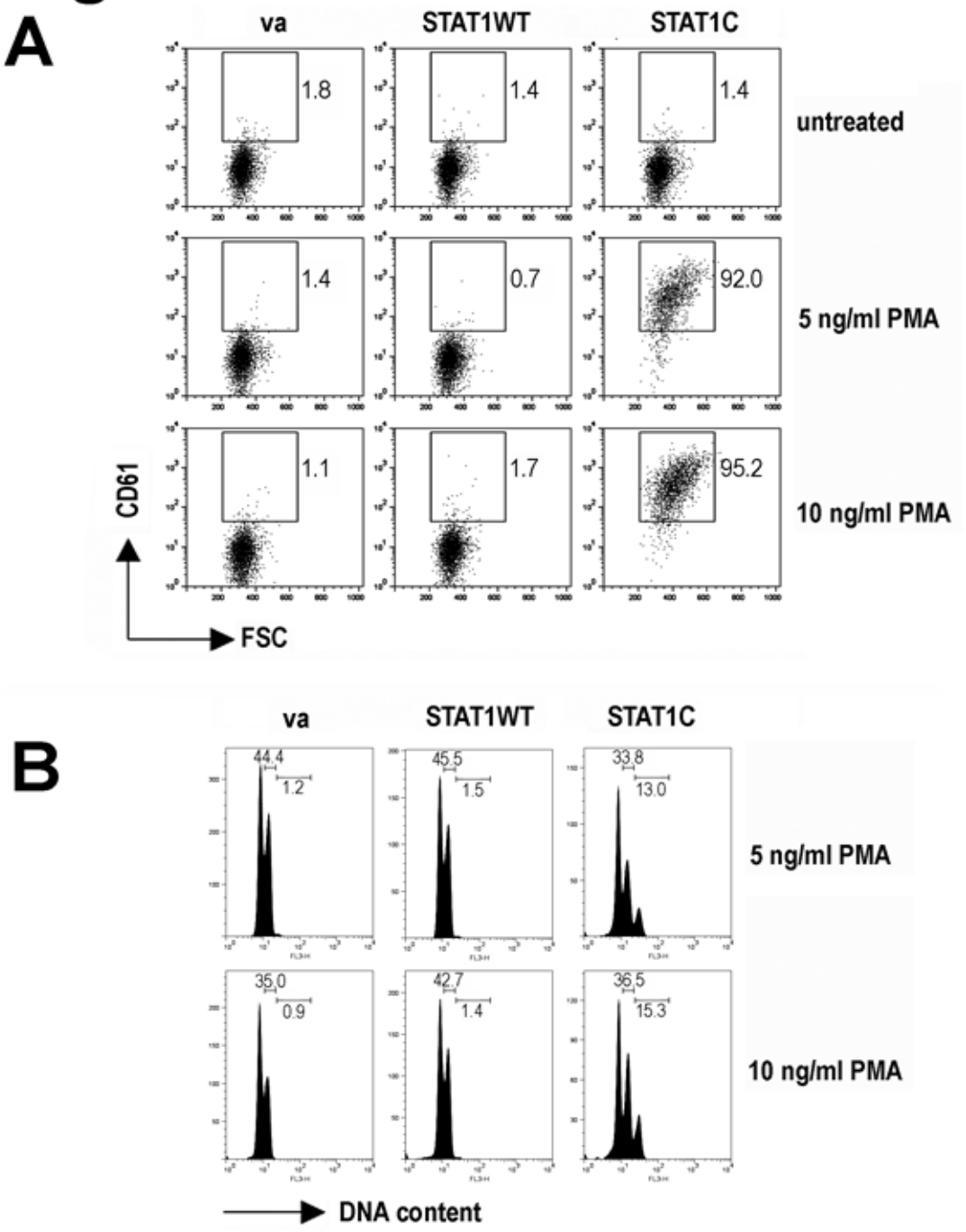

Figure S4, related to Figure 4.

(A) Representative FACS profiles showing increased numbers of CD61-expressing cells in the STAT1C-infected cultures following treatment with low doses of PMA. The data are representative of three independent experiments.

(B) Representative histograms depicting increased numbers of polyploid (>4n) cells in STAT1C-infected K562 cultures following treatment with low doses of PMA. The data are representative of three independent experiments.

Figure S5

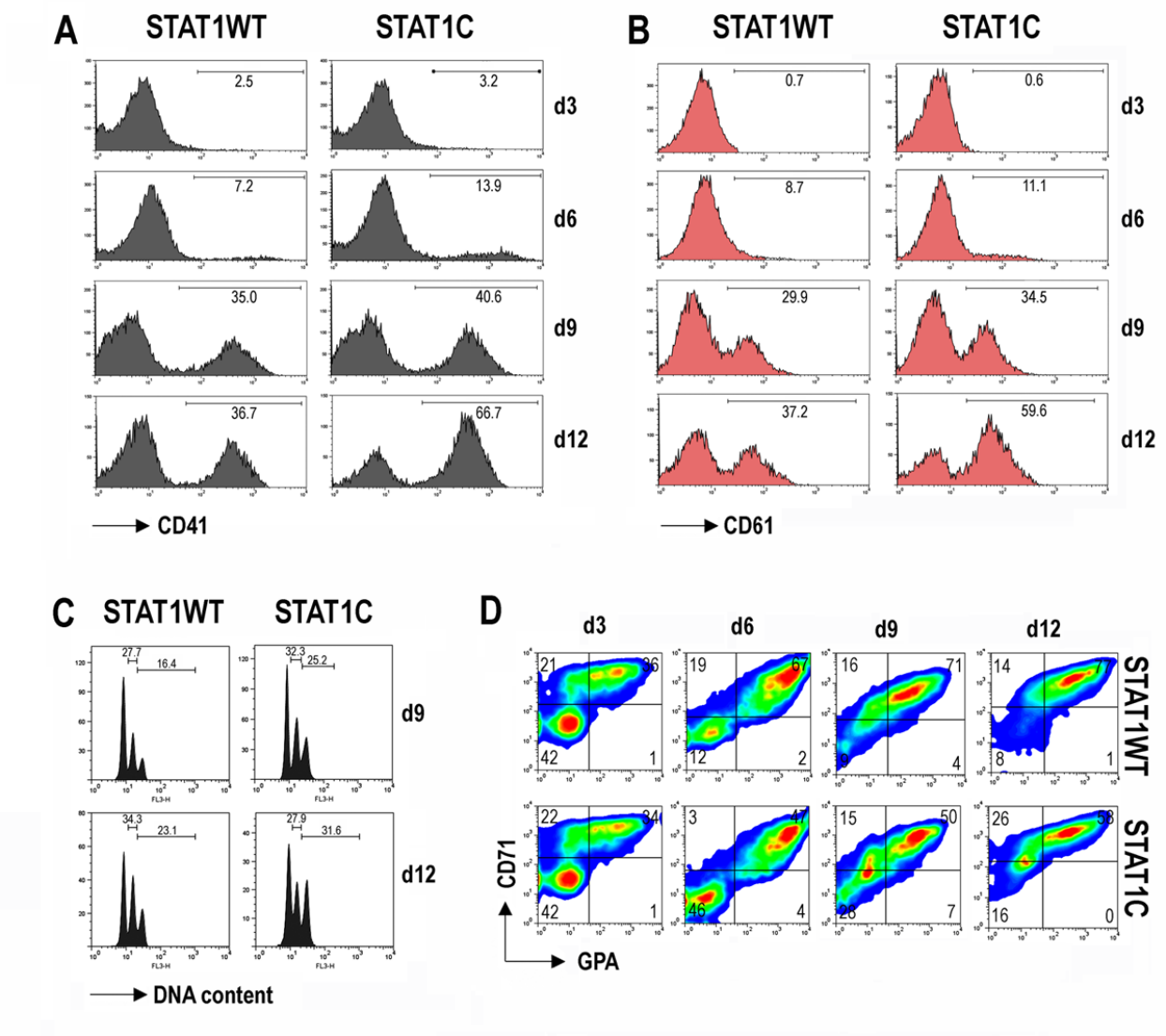

Figure S5, related to Figure 5.

(A) Representative FACS profiles showing increased CD41 cell surface expression and cell size analysis in constitutively active STAT1 (STAT1C)-transduced $CD34^{+}$ cells after 9 and 12 days of growth in media supporting megakaryocyte differentiation. The data are representative of 2 independent experiments.

(B) Representative FACS profiles showing increased CD61 cell surface expression and cell size analysis in STAT1C-transduced $CD34^+$ cells after 9 and 12 days of growth in media supporting megakaryocyte differentiation. The data are representative of 2 independent experiments.

(C) Histograms depicting increased numbers of polyploid (>4n) cells in constitutively active STAT1 (STAT1C)-transduced cord blood-derived $CD34^+$ cells following 9 and 12 days of growth in media supporting megakaryocyte differentiation. The data are representative of 2 independent experiments.

(D) Representative FACS profiles showing decreased glycophorin A (GPA) and CD71 cell surface expression in constitutively active STAT1 (STAT1C)-transduced cord blood derived $CD34^+$ cells following 9 and 12 days of growth in media supporting erythroid differentiation. The data are representative of 2 independent experiments.

SUPPLEMENTAL EXPERIMENTAL PROCEDURES

Expression profiling data processing

Fluorescent images were obtained using the Illumina Beadarray Reader, and fluorescence intensity data were extracted and quantified using Beadstudio. Data was subjected to background reduction, then filtered for those genes present in at least 75% of all samples, prior to standardization by quantiles normalization using the lumi package on R. Covariate adjustments for age, gender and treatment was performed using a linear regression model. Statistically significant interaction between V617F with each disease subtype were determined using Pinheiro's linear mixed effects (LME) package on R. The Storey q-value procedure was applied to control the false discovery rate (FDR) (Storey and Tibshirani, 2003). Hierarchical clustering was performed using Euclidean distance and complete linkage using the Cluster and Treeview software package. Gene set enrichment analysis (GSEA) was performed to analyze enrichment of gene sets following the developer's protocol (http://www.broad.mit.edu/gsea/), but using a more stringent FDR cut-off of 20% in view of the relatively small number of gene sets being analyzed.

Real-time quantitative PCR

Reverse transcription was performed on 100 ng total RNA using Superscript III (Invitrogen), and quantitative RT-PCR was performed using Brilliant SYBR Green QPCR Master Mix (Stratagene), according to manufacturer's protocols. The primers used for the PCR are: PIM1-fwd: CGAGCATGACGAAGAGATCAT; PIM1-rev: TCGAAGGTTGGCCTATCTGA; CISH-fwd: CTCCACAGCCAGCAAAGG; CISH-rev: CGGGCACACACATGTACCTA; IFI44L-fwd: CAGTTGCGCAGATGATTTTC; IFI44L-rev: CAATTTAAGCCTGATCTAACCCC; GBP2-fwd: GCAAGTTGATCTCTGGAGCC; GBP2-rev: GGACTCGACTTTCACATTGGA; IRF1-fwd: CTTCCATGGGATCTGGAAGA; IRF1-rev: GACCCTGGCTAGAGATGCAG; HLAF-fwd: GTGGCCTCATGGTCAGAGAT; HLAF-rev: GCTCCGCAGATACTTGGAGA; IFITM3-fwd: CCAACCATCTTCCTGTCCC, IFITM3-rev: ATGTCGTCTGGTCCCTGTTC; ACTIN-fwd: GTTGTCGACGACGAGCG; ACTIN-rev: GCACAGAGCCTCGCCTT. Results were calculated for each individual patient using the delta-delta-Ct method with β-actin as an internal control, and expressed as the ratio of expression of a given gene in the V617F-heterozygous sample to that in the corresponding wild-type samples. All PCRs were performed in triplicate.

Erythroid colony processing for flow cytometry, immunocytochemistry and immunoblotting

Individual BFU-E colonies grown in 0.01U/ml Epo were plucked into 100 μl PBS and stored on ice for no more than 4 h. For each colony, 5 μl was denatured at 95°C for 15 min to release cellular DNA, and genotyped and assigned JAK2 mutation statuses as described previously. Wild-type and V617F-heterozygous colonies were pooled, washed once in 1x PBS prior to downstream applications. For flow cytometry, pooled cells were staining for either CD71-PE (eBiosciences) and GPA-FITC (BD Biosciences), or fixed in 3% formaldehyde/MeOH prior to staining for intracellular pSTAT1 levels using an Alexafluor 488-conjugated pSTAT1 antibody (BD Biosciences). For pSTAT5 or pSTAT1 immunocytochemical staining, at least 3 colonies were cytospun onto glass slides and fixed in a 1:1 MeOH:acetone solution at -20°C overnight. Cells were subjected to blocking in 1% bovine serum albumin (BSA) in PBS + 0.05% Tween-20 (PBST), stained overnight with a pSTAT5- or pSTAT1-specific antibody (Cell Signaling), and visualized by staining with a phycoerythricin-conjugated anti-rabbit secondary antibody for 1 hour. Cells were also counter-stained with β-actin (Sigma) to visualize the cytoplasm and were mounted in a DAPI-containing mounting solution. Fluorescent micrographs were taken on a Zeiss Axioscop 2 fluorescent miscroscope. pSTAT5 or pSTAT1 staining was quantified for at least 50 individual cells using the Isis Imaging System (MetaSystems GmbH). Cells with >10% PE signal relative to DAPI were considered positive. For immunoblotting, equal numbers of wild-type and JAK2 mutant colonies were pooled and lysed directly into 2x SDS-PAGE loading buffer, denatured at 95°C for 5' and loaded directly onto acrylamide gels.

Cell line cultures and transfection

K562 cells were cultured in RPMI supplemented with 10% fetal calf serum, L-glutamine and penicillin/streptomycin. The JAK2-null γ2A cells were cultured in DMEM supplemented with 10% fetal calf serum. For IFNγ hypersensitivity assays, γ2A cells at ~50% confluency were transfected with JAK2-expressing constructs using Fugene 6 Transfection Reagent (Roche), and treated with 0, 1, 10 and 100 ng/ml IFNγ (R&D Systems) for 15 minutes.

Plasmid constructions and lentivirus production

STAT1-expressing constructs were generated by cloning the full length FLAG-STAT1 cDNA or the constitutively active FLAG-STAT1C cDNA (a kind gift from Dr. David Frank, Harvard University) into the PacI site of the pLKO.3G vector. The STAT1 dominant negative (STAT1DN) construct was made by replacing the STAT1 Tyr701 in the pLKO.3G-STAT1 plasmid with a phenylalanine residue using the QuikChange XL kit (Stratagene). All clones were subsequently sequenced to ensure no additional mutations were present. Viral supernatants were produced by co-transfecting the pLKO.3G-STAT1 constructs into 293T packaging cell line along with two helper plasmids, psPAX2 and pMD2.G,

supernatants were collected following 24h and 48h, and concentrated by ultracentrifugation at 28,000 rpm for 2 h.

K562 differentiation assays

K562 cells were cultured in RPMI supplemented with 10% fetal calf serum. Cells in log phase were infected by STAT1-expressing lentiviruses by spinoculation for 2h in the presence of 4 μg/ml polybrene. K562 cells were differentiated into erythroid and megakaryocytic lineages using 50 μM hemin and 50 ng/ml PMA, respectively. DNA content analysis, benzidine staining and GpIX and γ-globin expression on differentiated K562 cells were performed as previously described (Huo et al., 2006).

Cord blood $CD34^+$ MNC purification and erythroid/megakaryocytic differentiation

Cord blood $CD34^+$ differentiation was performed as previously described (Ugo et al., 2004) with modifications. Cord blood mononuclear cells were obtained from cord blood over a ficoll gradient, and $CD34^+$ cells were selected using a magnetic cell sorting system (Miltenyi Biotec), according to the manufacturer's protocols. The purity of recovered cells was always greater than 90% as determined by flow cytometry. Purified $CD34^+$ cells were expanded ex vivo in SFEM medium supplemented with 100 ng/ml Flt3 ligand and 10 ng/ml recombinant human thrombopoietin (rhTPO) for 2 days, followed by infection with STAT1-expressing lentiviruses by spinoculation for 2h in the presence of 4 μg/ml polybrene. Cells were seeded at $1x10^4$ cells/well of a 24-well dish, and cultured with SFEM medium supplemented with 25 ng/ml recombinant human stem cell factor (rhSCF), 0.5 U/ml recombinant human erythropoietin (rhEPO), 30 μg/ml holo-transferrin, 10 nM β-mercaptoethanol and 4 μg/ml dexamethasone to induce erythroid differentiation, or SFEM supplemented with 25 ng/ml rhSCF, 100 ng/ml rhTPO to induce megakaryocyte differentiation. At day 6, cells were transferred to a 6-well dish and supplemented with fresh media. For flow cytometry analysis, cells were taken at day 3, 6, 9 and 12, and stained with GPA and CD71 to detect erythroid cells, and with CD41 or CD61 to quantify megakaryocytes. For real-time qPCR analysis, GFP^+ cells were sorted at day 9 and 12 using a FACS Vantage cytometer (Becton-Dickinson) equipped with an argon laser.

Western blot analyses

Western blot analyses were performed on total cell lysates using the following antibodies: anti-JAK2 (Imgenex), anti-pY701-STAT1 (Cell Signaling), anti-STAT1 (Santa Cruz), pSTAT5 (Cell Signaling), anti-pY694-STAT5 (Santa Cruz) and anti-β-actin (Sigma).

SUPPLEMENTAL REFERENCES

Huo, X. F., Yu, J., Peng, H., Du, Z. W., Liu, X. L., Ma, Y. N., Zhang, X., Zhang, Y., Zhao, H. L., and Zhang, J. W. (2006). Differential expression changes in K562 cells during the hemin-induced erythroid differentiation and the phorbol myristate acetate (PMA)-induced megakaryocytic differentiation. Mol Cell Biochem *292*, 155-167.

Storey, J. D., and Tibshirani, R. (2003). Statistical significance for genomewide studies. Proc Natl Acad Sci U S A *100*, 9440-9445.

Ugo, V., Marzac, C., Teyssandier, I., Larbret, F., Lecluse, Y., Debili, N., Vainchenker, W., and Casadevall, N. (2004). Multiple signaling pathways are involved in erythropoietin-independent differentiation of erythroid progenitors in polycythemia vera. Exp Hematol *32*, 179-187.